pyridyl ligand. Such variations necessarily lead to perturbations in the basic chromophore but offer some obvious advantages. One, in particular, in terms of excited-state redox potentials, is the possibility of manipulating potentials of the excited states as reductants, by varying the π^* levels of the chromophoric ligand. Such variations will be the subject of a forthcoming publication.[37]

Acknowledgment is made to the Department of Energy under Grant No. DE-AS05-78EE06034 for support of this research.

Registry No. **1**, 85452-91-1; **2**, 79968-44-8; **3**, 31067-98-8; **4**, 80502-77-8; **5**, 80558-59-4; **6**, 75441-72-4; **7**, 75446-24-1; **8**, 75446-26-3; **9**, 96964-76-0; **10**, 80502-69-8; **11**, 89711-31-9; **12**, 96964-77-1; **13**, 15158-62-0; $(phen)Os(py)_4^{2+}$, 80502-71-2; $(phen)_2Os(py)_2^{2+}$, 80502-73-4; $(phen)_2Os(das)^{2+}$, 96964-78-2; $(phen)_2Os(dppb)^{2+}$, 96964-79-3; $(phen)_2Os(dpae)^{2+}$, 80502-85-8; $(phen)_2Os(dppe)^{2+}$, 80502-83-6; $(phen)Os(das)_2^{2+}$, 80502-87-0; $(phen)Os(dppene)_2^{2+}$, 96964-80-6; BZQ^{2+}, 13096-46-3; PQ^{2+}, 4685-14-7; Mepy-$4CN^+$, 13441-45-7; Mepy-$4CO_2Me^+$, 38117-49-6; Etpy-$4CO_2Me^+$, 48128-20-7; Etpy-$4CONH_2^+$, 71258-88-3; Mepy-$4CONH_2^+$, 45791-94-4; Bzpy-$3CONH_2^+$, 16183-83-8; Etpy-$3CONH_2^+$, 71413-64-4; Mepy-$3CONH_2^+$, 3106-60-3; TMPD, 100-22-1; TMBD, 366-29-0; 3-MeO-PTZ, 1771-19-3; PTZ, 92-84-2; 4-MeO-DMA, 701-56-4; 2-Cl-PTZ, 92-39-7; 2-CF_3-PTZ, 92-30-8; 4-Me-DMA, 99-97-8; 10-Me-PTZ, 1207-72-3; DMA, 121-69-7; 4-Br-DMA, 586-77-6; TPA, 603-34-9; TBTPA, 4316-58-9; PXT, 262-20-4.

Supplementary Material Available: Tables of redox potentials for 10 oxidative quenchers and 14 reductive quenchers and tables of oxidative and reductive quenching rate constants for a series of Os(II) MLCT excited states (4 pages). Ordering information is given on any current masthead page.

---

(37) Johnson, S.; Westmoreland, T. D.; Kober, E. M.; Sullivan, B. P.; Caspar, J. V.; Meyer, T. J., manuscript in preparation.

Contribution from the Departments of Chemistry, University of Santa Clara,
Santa Clara, California 95053, and University of Colorado, Boulder, Colorado 80309

First-Row Transition-Metal Complexes of Pyridine-2,6-dicarboxylic Acid *N*-Oxide. Crystal Structure of Diaqua(pyridine-2,6-dicarboxylate *N*-oxido)manganese(II)

LAWRENCE C. NATHAN,*[†] CHRISTINE A. DOYLE,[†] ANNE M. MOORING,[†] DONALD C. ZAPIEN,[†] SCOTT K. LARSEN,[‡] and CORTLANDT G. PIERPONT[‡]

Received July 9, 1984

Five complexes with general formula $M(pdcO)(H_2O)_2$ (where $pdcO^{2-}$ is the pyridine-2,6-dicarboxylate *N*-oxide ion and M^{2+} is Mn, Co, Ni, Cu, and Zn) have been synthesized and characterized by elemental analyses, infrared and electronic absorption spectroscopy, and magnetic susceptibility measurements. The crystal structure of $Mn(C_7H_3NO_5)(H_2O)_2$ was determined. The complex is polymeric with manganese six-coordinated to two bridging *N*-oxide groups (trans), two terminal carboxyl groups (cis), and two water molecules (cis). Crystal data: orthorhombic, space group *Pcca*, $a = 8.005$ (1) Å, $b = 6.334$ (2) Å, $c = 18.673$ (4) Å, $Z = 4$, $R = 0.0363$, 1030 reflections. X-ray powder diffraction patterns indicate that all five complexes are not isomorphous.

Introduction

Although the coordinating properties of heterocyclic amine *N*-oxides have been the subject of three review articles,[1-3] the ligand pyridine-2,6-dicarboxylic acid *N*-oxide (hereafter abbreviated as H_2pdcO) has received virtually no attention. This unique ligand was of interest for several reasons. First, its parent amine, pyridine-2,6-dicarboxylic acid (also known as dipicolinic acid), has been thoroughly studied and is known to coordinate unpredictably as the neutral molecule, the univalent anion, or the divalent anion, bidentate in some cases and tridentate in others.[4-7] Second, while essentially all reported *N*-oxide complexes are neutral or cationic,[1-3] H_2pdcO may form anionic *N*-oxide complexes. Third, H_2pdcO may form binuclear or polymeric complexes with first-row transition-metal ions. We are aware of only one report of a complex of H_2pdcO, namely $UO_2(pdcO)\cdot 3H_2O$, which is dimeric with tridentate $pdcO^{2-}$ ligands in which the *N*-oxide oxygen and one carbonyl group coordinate to one uranium while the remaining carboxyl group is coordinated to the second uranium.[8]

Experimental Section

Synthesis of Pyridine-2,6-dicarboxylic Acid *N*-Oxide, $C_7H_5NO_5$ (H_2pdcO). The ligand H_2pdcO was prepared in 66% yield by hydrogen peroxide oxidation of the parent amine by the method of Syper and co-workers.[9] The extraction step was done with a continuous liquid extractor. Mp: 157–159 °C (lit.[9] mp 158–160 °C).

Synthesis of the Complexes. A 25-mL aliquot of a hot aqueous solution containing 5 mmol of pyridine-2,6-dicarboxylic acid *N*-oxide was added with stirring to 25 mL of hot aqueous solution containing 5 mmol of the appropriate hydrated metal acetate, $M(C_2H_3O_2)_2\cdot nH_2O$ (M = Mn, Co, Ni, and Cu and $n = 4$; M = Zn and $n = 2$). Except for the manganese complex, the product precipitated almost immediately. The manganese complex was obtained by reducing the volume of water and allowing the solution to cool overnight. The products were filtered, washed with small portions of cold water, and dried under vacuum over phosphorus pentoxide. Yields of the $M(pdcO)(H_2O)_2$ complexes ranged from 70 to 100%. **$MnC_7H_7O_7N$**: yellow; dec pt 257–263 °C. Anal. Calcd: C, 30.90; H, 2.59; N, 5.15. Found: C, 30.94; H, 2.72; N, 5.07. **$CoC_7H_7O_7N$**: pink; dec pt 235–238 °C. Anal. Calcd: C, 30.45; H, 2.56; N, 5.07. Found: C, 30.25; H, 2.70; N, 4.95. **$NiC_7H_7O_7N$**: green; dec pt 265–270 °C. Anal. Calcd: C, 30.48; H, 2.56; N, 5.08. Found: C, 30.54; H, 2.68; N, 5.04. **$CuC_7H_7O_7N$**: blue; dec pt 268–271 °C. Anal. Calcd: C, 29.95; H, 2.51; N, 4.99. Found: C, 29.75; H, 2.63; N, 4.90. **$ZnC_7H_7O_7N$**: white; dec pt 240–242 °C. Anal. Calcd: C, 29.76; H, 2.50; N, 4.96. Found: C, 29.62; H, 2.77; N, 4.85.

Physical and Spectral Measurements. Magnetic susceptibility measurements were done on solid samples by the Gouy method at 296–297 K and 5400 G. $HgCo(SCN)_4$ was used as calibrant. Diamagnetic corrections were made by using Pascal's constants. The temperature-independent paramagnetism correction of 60×10^{-6} cgsu was used for the copper complex. The pooled standard deviation from up to five replicate measurements on each compound was 0.05 μ_B. Due to the insolubility of the complexes, electronic absorption spectra were obtained on solid samples as Nujol mulls on Cary 14 and Beckman DBGT spectrophotometers. Infrared spectra were obtained as KBr pellets and as Nujol mulls on a Beckman IR-8 spectrophotometer. X-ray powder diffraction data were obtained by using a Diano XRD-8000 semiauto-

---

[†] University of Santa Clara.

[‡] University of Colorado.

(1) Orchin, M.; Schmidt, P. J. *Coord. Chem. Rev.* **1968**, *3*, 345.

(2) Garvey, R. G.; Nelson, J. H.; Ragsdale, R. O. *Coord. Chem. Rev.* **1968**, *3*, 375.

(3) Karayannis, N. M.; Pytlewski, L. L.; Mikulski, C. M. *Coord. Chem. Rev.* **1973**, *11*, 93.

(4) Furst, W.; Gouzenh, P.; Jeannin, Y. *J. Coord. Chem.* **1978**, *8*, 237.

(5) Fowles, G. W. A.; Matthews, R. W.; Walton, R. A. *J. Chem. Soc. A* **1968**, 1108.

(6) Chiesi Villa, A.; Guastini, C.; Musatti, A.; Nardelli, M. *Gazz. Chim. Ital.* **1972**, *102*, 226.

(7) Biagini, M.; Chiesi Villa, A.; Guastini, C.; Nardelli, M. *Gazz. Chim. Ital.* **1972**, *102*, 1026.

(8) Bombieri, G.; Degetto, S.; Forsellini, E.; Marangoni, G.; Immirzi, A. *Cryst. Struct. Commun.* **1977**, *6*, 115.

(9) Syper, L.; Kloc, K.; Mlochowski, J.; Szulc, Z. *Synthesis* **1979**, 521.

0020-1669/85/1324-2763$01.50/0

Table I. Crystal Data and Details of the Structure Determination for $[Mn(pdcO)(H_2O)_2]_n$

Crystal Data	
formula	$MnC_7H_7NO_7$
mol wt	272.01
color	yellow
space group[a]	*Pcca*
cryst syst	orthorhombic
a, Å[b]	8.005 (1)
b, Å	6.334 (2)
c, Å	18.673 (4)
α, deg	90.00
β, deg	90.00
γ, deg	90.00
V, Å^3	946.8 (4)
d_{obsd}, g cm^{-3}	1.86 (2)
Z	4
d_{calcd}, g cm^{-3}	1.91
F(000)	548
μ, cm^{-1}	13.59
cryst dimens, mm	0.18 × 0.24 × 0.37
Data Collection and Reduction	
diffractometer	Syntex P$\bar{1}$
data collcd	+*h*,+*k*,+*l*
radiation	Mo Kα (λ = 0.71069 Å)
monochromator angle, deg	12.2
temp, K	294–296
scan technique	θ–2θ
scan range (2θ) min–max, deg	3.0–50.0
scan speed, deg/min	4.0
scan range	0.7° below Kα_1 and 0.7° above Kα_2
bkgd	stationary cryst–stationary counter bkgd time = 0.5(scan time)
check reflcns	(214), (430), (124)
frequency	every 100 measurements
variation	random, 4.5%
no. of unique reflcns measd	1030
no. of obsd reflcns	673
criterion	$F > 6\sigma(F)$
abs cor	none
Structure Determination and Refinement	
method of phase determination	SHELX[c]
scattering factors	neutral atoms[d]
R_1, R_2[e]	0.0363, 0.0414
wt	$1/(\sigma(F)^2 + 0.001F^2)$
no. of params	89
ratio of observns to params	7.54
max shift/error (non-hydrogen)	0.81
residual electron density, e/Å^3	0.5

[a] "International Tables for X-ray Crystallography"; Kynoch Press: Birmingham, England, 1965; Vol. 1. [b] Cell dimensions were determined by a least-squares fit of the setting angles of 15 reflections with 2θ in the range 15–25°. [c] Sheldrick, G. M. SHELX76, A Program for Crystal Structure Determination, University of Cambridge, England. [d] "International Tables for X-ray Crystallography"; Kynoch Press: Birmingham, England, 1974; Vol. 4, pp 55–60, 99–101, 149–150. [e] The quantity minimized in the least-squares procedures is $\sum w(|F_o| - |F_c|)^2$. $R_1 = \sum||F_o| - |F_c||/\sum|F_o|$; $R_2 = [\sum w(|F_o| - |F_c|)^2/\sum w|F_o|^2]^{1/2}$.

matic diffractometer and Cu Kα radiation. Single-determination elemental analyses were done by M-H-W Laboratories, Phoenix, AZ.

Structure Determination of $[Mn(pdcO)(H_2O)_2]_n$. A parallelepiped-shaped crystal grown from aqueous solution was mounted and aligned on a Syntex P$\bar{1}$ automated diffractometer. Preliminary photographs and subsequent data collection (summarized in Table I) indicated orthorhombic symmetry with the unit cell defined in the table. Systematic absences uniquely implied space group *Pcca*. The density and unit-cell volume indicated *Z* = 4 and hence a special site and symmetry for the complex. In the structure solved by using MULTAN-78, the pyridine rings lie on the 2-fold axis along *c* and the manganese ions lie on the 2-fold axis along *b*. Refinement of the positions of all independent atoms with anisotropic thermal parameters for non-hydrogen atoms converged to the values in Table II, with $R_1 = 0.0363$ and $R_2 = 0.0414$. ψ scans indicated that absorption effects were not significant, and no correction was performed. Supplementary material includes tables of F_o, F_c, and anisotropic thermal parameters and a stereoview of the unit cell.

Table II. Positional and Isotropic Thermal Parameters for $[Mn(pdcO)(H_2O)_2]_n$

atom	*x*	*y*	*z*	U_{iso},[a] Å^2
Mn	0.0	0.5203 (1)	0.25	0.0197 (3)
O(1)	0.25	0.5	0.3061 (2)	0.021 (1)
O(2)	−0.0429 (3)	0.2732 (4)	0.3256 (1)	0.030 (1)
O(3)	0.0438 (4)	0.0166 (4)	0.3968 (2)	0.040 (1)
O(4)	−0.1185 (3)	0.7446 (5)	0.3176 (2)	0.039 (1)
N	0.25	0.5	0.3778 (2)	0.017 (1)
C(1)	0.0487 (4)	0.1980 (5)	0.3735 (2)	0.022 (1)
C(2)	0.1632 (4)	0.3489 (6)	0.4132 (2)	0.019 (1)
C(3)	0.1685 (5)	0.3452 (7)	0.4873 (2)	0.024 (1)
C(4)	0.25	0.5	0.5247 (3)	0.027 (1)
H(1)	0.112 (6)	0.234 (8)	0.508 (3)	0.043 (13)
H(2)	0.25	0.5	0.585 (4)	0.065 (24)

[a] Equivalent isotropic thermal factor calculated as the average of the orthogonal diagonal matrix elements of the U_{ij} tensor: Hamilton, W. C. *Acta Crystallogr.* **1959**, *12*, 609.

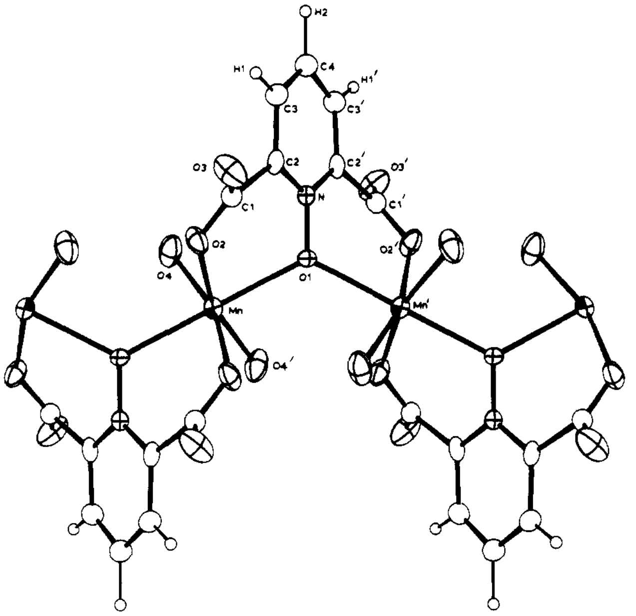

Figure 1. View of the repeating complex unit of polymeric $[Mn(pdcO)(H_2O)_2]_n$ down the crystallographic *b* axis.

Results and Discussion

The complexes produced by reacting the various metal acetates with H_2pdcO according to reaction 1 are insoluble in common

$$M(C_2H_3O_2)_2 \cdot nH_2O + H_2pdcO \xrightarrow{H_2O} M(pdcO)(H_2O)_2 + 2HC_2H_3O_2 + (n-2)H_2O \quad (1)$$

organic solvents. Attempts to prepare anionic complexes according to reaction 2 resulted in the same $M(pdcO)(H_2O)_2$ products.

$$M(C_2H_3O_2)_2 \cdot nH_2O + 2NaOH + 2H_2pdcO \xrightarrow{H_2O} Na_2[M(pdcO)_2] + 2HC_2H_3O_2 + nH_2O \quad (2)$$

Crystallographic results for $Mn(pdcO)(H_2O)_2$ presented in Figure 1 and Table III indicate that polymeric complex chains of alternating Mn^{2+} and $pdcO^{2-}$ ions extend along *a*. Each *N*-oxide oxygen atom bridges two Mn^{2+} ions while each carboxylate group bonds terminally through a single oxygen atom. This results in a nonplanar six-membered chelate ring at each metal. While rotation of the carboxylate groups by 44.7° from the plane of the pyridine ring increases the bite of the ligand, the O(1)–Mn–O(2) bond angle remains quite contracted (78.2°) because the Mn–O bond lengths, while typical of Mn^{2+} complexes,[10] are much longer than the other ring bond lengths. In the manganese octahedron the *N*-oxide oxygens are trans, the carboxylate oxygens cis, and

---

(10) Lynch, M. W.; Hendrickson, D. N.; Fitzgerald, B. J.; Pierpont, C. G. *J. Am. Chem. Soc.* **1984**, *106*, 2041.

Table III. Selected Bonding Parameters for $[Mn(pdcO)(H_2O)_2]_n$

	Bond Lengths (Å)		
Mn–O(1)	2.262 (1)	N–C(2)	1.355 (4)
Mn–O(2)	2.135 (3)	O(3)–C(1)	1.229 (4)
Mn–O(4)	2.124 (3)	C(1)–C(2)	1.517 (5)
N–O(1)	1.339 (5)	C(2)–C(3)	1.385 (5)
O(2)–C(1)	1.252 (4)	C(3)–C(4)	1.369 (5)
C(3)–H(1)	0.92 (5)	C(4)–H(2)	1.13 (7)
	Bond Angles (deg)[a]		
Mn–O(1)–Mn′	124.9 (1)	N–O(1)–Mn	117.6 (1)
O(1)–Mn–O(2)	78.2 (1)	C(1)–O(2)–Mn	131.1 (2)
O(1)–Mn–O(4)	99.1 (1)	C(2)–N–O(1)	119.2 (2)
O(1)–Mn–O(1)″	174.1 (2)	O(3)–C(1)–O(2)	126.1 (3)
O(1)–Mn–O(2)′	97.0 (1)	C(2)–C(1)–O(2)	117.6 (3)
O(1)–Mn–O(4)′	85.3 (1)	C(2)–C(1)–O(3)	115.9 (3)
O(2)–Mn–O(4)	91.5 (1)	C(1)—C(2)–N	121.1 (3)
O(2)–Mn–O(2)′	85.7 (2)	C(3)–C(2)–N	118.9 (3)
O(2)–Mn–O(4)′	162.7 (1)	C(1)–C(2)–C(3)	119.7 (3)
O(4)–Mn–O(4)′	96.0 (2)	C(2)–C(3)–C(4)	120.8 (4)

[a] Primed and double primed atoms are related to those in Table II by the symmetry transformations $^1/_2 - x, -y, z$ and $^1/_2 + x, -y, -z$, respectively.

Table IV. Selected Infrared Band Positions (cm^{-1})[a]

	stretching band		
compd	O–H[b]	carboxyl	N–O
H_2pdcO	2520 m, br	1724 s, br	1250 m
		1324 s	1168 s
$Mn(pdcO)(H_2O)_2$	3367 s, br	1631 s, br	1245 m–s
	2985 s	1359 s, br	1190 m–s
$Co(pdcO)(H_2O)_2$	3378 s, br	1650 s, br	1248 m
	3195 sh	1351 s	1193 m
$Ni(pdcO)(H_2O)_2$	3356 s, br	1639 s, br	1242 m
	3184 sh	1355 s	1190 m
$Cu(pdcO)(H_2O)_2$	3395 s, br	1590 s, br	1252 m
	3096 s	1376 s	1195 m–s
$Zn(pdcO)(H_2O)_2$	3344 s, br	1645 s, br	1245 m
	3145 sh	1346 s, br	1198 m

[a] KBr pellets except for the zinc complex (Nujol mull); s = strong, m = medium, sh = shoulder, br = broad. [b] Intramolecular hydrogen-bonded O–H for H_2pdcO; coordinated water for complexes.

the water molecule oxygens cis. O(2)–O(4′) separations of 2.717 (4) Å and imposed crystallographic symmetry provide the proper orientation for hydrogen bonds between aquo ligands of one metal and coordinated carboxylate oxygen atoms of an adjacent complex unit. Structural features of the $pdcO^{2-}$ ligand are similar to those of free H_2pdcO with the following exceptions: the H_2pdcO carboxyl groups were found to be essentially coplanar with the pyridine ring, there was a larger difference between H_2pdcO carboxyl C–O bond lengths,[11] indicating greater delocalization over both C–O bonds in the manganese complex, and carboxyl hydrogen atoms were oriented toward the *N*-oxide oxygen atom, suggesting a strong hydrogen-bonding interaction. One other complex of $pdcO^{2-}$ has been reported.[8] While the $[UO_2(pdcO)(H_2O)_2]_2$ dimer also contains bridging $pdcO^{2-}$ ligands, the nature of the bridge is different from that for $[Mn(pdcO)(H_2O)_2]_n$, as illustrated in I and II.

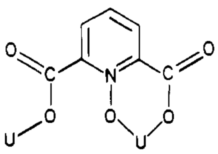

I

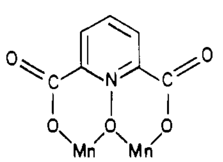

II

Infrared spectra of all five complexes are very similar to one another yet distinctly different from the spectrum of the free ligand. Some of the more relevant bands are listed in Table IV.

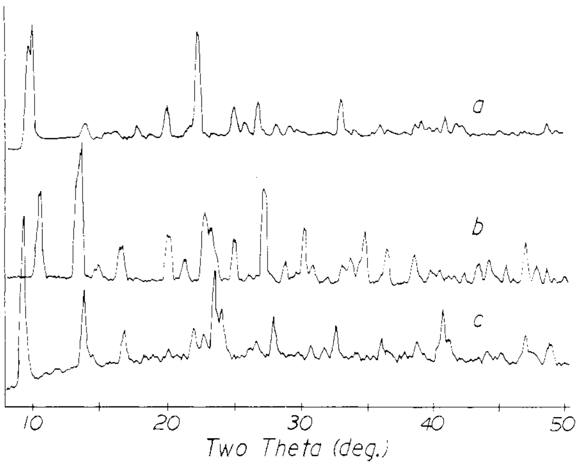

Figure 2. X-ray powder diffraction patterns for $M(pdcO)(H_2O)_2$ complexes where M is (a) Cu, (b) Zn, or (c) Mn.

Table V. Magnetic Susceptibility and Electronic Spectral Data

complex	μ_{eff}, μ_B	abs max $10^{-3}\bar{\upsilon}$, cm^{-1}	band assgnt	calcd ligand field params Dq, cm^{-1}	calcd ligand field params B, cm^{-1}
$Mn(pdcO)(H_2O)_2$	5.88	26.2			
		19.2 sh			
$Co(pdcO)(H_2O)_2$	4.75	20.7	$^4T_{1g}(P) \leftarrow {}^4T_{1g}(F)$	984	879
		18.2	$^4A_{2g} \leftarrow {}^4T_{1g}(F)$		
		8.77	$^4T_{2g} \leftarrow {}^4T_{1g}(F)$		
$Ni(pdcO)(H_2O)_2$	2.97	26.9	$^3T_{1g}(P) \leftarrow {}^3A_{2g}$	907	975
		15.0	$^3T_{1g}(F) \leftarrow {}^3A_{2g}$		
		13.7 sh			
		9.07	$^3T_{2g} \leftarrow {}^3A_{2g}$		
$Cu(dpcO)(H_2O)_2$	2.03	13.6	$^2T_{2g} \leftarrow {}^2E_g$	1360	

The band due to intramolecular hydrogen-bonded OH groups in the free ligand is replaced by bands due to coordinated water. For the complexes, bands attributable to the carboxyl moiety are found at positions consistent with coordination via this functional group.[12] While most substituted pyridine *N*-oxides have a single N–O band in the 1300–1200-cm^{-1} region,[13] H_2pdcO is similar to 2-substituted pyridine *N*-oxides with electron-withdrawing substituents, which commonly have two such bands.[12,14] Typically, a decrease of 10–70 cm^{-1} is observed in these N–O bands upon coordination.[12,13] While the data in Table IV do not demonstrate this typical behavior, the decrease expected in ν_{NO} upon coordination might be offset by a simultaneous increase due to disruption of the strong hydrogen-bonding interaction within the free ligand. Similar behavior was observed[15] for some complexes of 2-aminopyridine *N*-oxide where ν_{NO} was reported in the 1211–1178-cm^{-1} region as compared to the free ligand value of 1192 cm^{-1}. Finally, the KBr sample preparation technique apparently decomposes at least some of the $Zn(pdcO)(H_2O)_2$ complex, as the infrared spectrum in this medium has bands typical of both the complex and the free ligand. The Nujol mull technique gave a spectrum of the zinc complex that was consistent with those of the other four complexes.

Despite the similarities of the infrared spectra, X-ray powder diffraction patterns demonstrate that only the cobalt, nickel, and zinc complexes are isomorphous. Apparently the manganese and copper complexes have unique structures. Representative patterns are shown in Figure 2. Patterns for the cobalt and nickel complexes are very similar to the one shown for zinc in terms of peak position and intensity.

Although the crystallographic data show the manganese coordination octahedron to be fairly distorted, electronic spectra of

---

(11) Rychlewski, U.; Gdaniec, M. *Acta Crystallogr., Sect. B: Struct. Crystallogr. Cryst. Chem.* **1977**, *B33*, 3555.

(12) Lever, A. B. P.; Lewis, J.; Nyholm, R. S. *J. Chem. Soc.* **1962**, 5262.

(13) Nathan, L. C.; Ragsdale, R. O. *Inorg. Chim. Acta* **1974**, *10*, 177.

(14) Katritzky, A. R.; Hands, A. R. *J. Chem. Soc.* **1958**, 2195.

(15) Landers, A. E.; Phillips, D. J. *Inorg. Chim. Acta* **1983**, *74*, 43.

the cobalt, nickel, and copper complexes (Table V) did not show any features that would indicate significant distortion of their coordination octahedra. The spectra were analyzed by assuming octahedral symmetry about the metal ions, and back-calculation of band positions from the best-fit values of *Dq* and *B* gave good agreement (less than 1.5% error for cobalt, less than 0.5% error for nickel) with the experimental band positions. The nickel complex displays the typical double ν_2 band associated with the mixing of the ^1E_g and $^3T_{1g}(F)$ energy levels. *Dq* values for the $M(pdcO)(H_2O)_2$ complexes are somewhat higher than those reported for six-coordinate complexes of various substituted pyridine *N*-oxides, most of which have *Dq* values in the ranges of 890–950 cm^{-1} for cobalt(II), 780–833 cm^{-1} for nickel(II), and 1220 cm^{-1} for copper(II).[3]

Ambient-temperature magnetic measurements (Table V) are consistent with six-coordination about the central metal ions and, with the exception of the 2.97 μ_B value for $Ni(pdcO)(H_2O)_2$, are consistent with values previously reported for six-coordinate complexes of other substituted pyridine *N*-oxides: 5.88–5.93 μ_B for manganese(II),[16,17] 4.71–4.84 μ_B for cobalt(II),[18] 3.30–3.34 μ_B for nickel(II),[18] and 1.91 μ_B for copper(II).[18] Manganese(II) complexes such as $Mn(py\text{-}N\text{-}O)Cl_2$ ((py-*N*-O) = pyridine *N*-oxide) for which chlorine-bridged structures are proposed have μ_{eff} values in the 5.40–5.60-μ_B range.[3] Monomeric copper(II) complexes with *N*-oxide ligands exhibit μ_{eff} values in the 1.75–2.04-μ_B range while dimeric copper(II) complexes have values as low as 0.22 μ_B resulting from strong spin–spin coupling.[19] A value of 0.85 μ_B has been reported for $Cu(py\text{-}N\text{-}O)Cl_2$, which is known to have an *N*-oxide-bridged dimeric structure.[20] Therefore, the μ_{eff} values for the $M(pdcO)(H_2O)_2$ complexes suggest no significant spin–spin coupling. The Mn–Mn′ separation of 4.011 (1) Å precludes any possibility of direct interaction between metal ions.

Typical of the other manganese(II) pyridine *N*-oxide complexes, $Mn(pdcO)(H_2O)_2$ is sensitive to visible light and its color changes over time from yellow to brown. Such changes have been attributed to a photooxidation–photoreduction process that produces manganese(III) and the parent amine.[21]

Acknowledgment. The authors thank the Chemistry Department, San Jose State University, for the use of their XRD-8000 instrument.

Registry No. $Mn(pdcO)(H_2O)_2$, 97277-46-8; $Co(pdcO)(H_2O)_2$, 97277-47-9; $Ni(pdcO)(H_2O)_2$, 97277-48-0; $Cu(pdcO)(H_2O)_2$, 97277-49-1; $Zn(pdcO)(H_2O)_2$, 97277-50-4.

Supplementary Material Available: A listing of observed and calculated structure factors, a table of anisotropic thermal parameters, and a stereoview of the unit cell of $[Mn(pdcO)(H_2)_2]_n$ (5 pages). Ordering information is given on any current masthead page.

---

(16) Carlin, R. L. *J. Am. Chem. Soc.* **1961**, *83*, 3773.

(17) Byers, W.; Lever, A. B. P.; Parish, R. V. *Inorg. Chem.* **1968**, *7*, 1835.

(18) Whyman, R.; Hatfield, W. E.; Paschal, J. S. *Inorg. Chim. Acta* **1967**, *1*, 113.

(19) Watson, W. H. *Inorg. Chem.* **1969**, *8*, 1879.

(20) Sager, R. S.; Williams, R. J.; Watson, W. H. *Inorg. Chem.* **1967**, *6*, 951.

(21) Nathan, L. C.; Cullen, J.; Ragsdale, R. O. *Inorg. Nucl. Chem. Lett.* **1976**, *12*, 137.

Contribution from the Departments of Chemistry, Oregon State University,
Corvallis, Oregon 97331, and University of Texas, Austin, Texas 78712

Structure and Bonding in Transition-Metal Carbonyls and Nitrosyls. 1. Gas-Phase Electron Diffraction Investigations of Tetranitrosylchromium ($Cr(NO)_4$), Carbonyltrinitrosylmanganese ($MnCO(NO)_3$), and Dicarbonyldinitrosyliron ($Fe(CO)_2(NO)_2$)

LISE HEDBERG,[1a] KENNETH HEDBERG,*[1a] SUSHIL K. SATIJA,[1b] and BASIL I. SWANSON[1c]

Received October 26, 1984

The molecular structures of gaseous $Cr(NO)_4$, $MnCO(NO)_3$, and $Fe(CO)_2(NO)_2$ have been investigated by electron diffraction at nozzle-tip temperatures of 29–37, 19–30, and 23 °C, respectively. The molecules have tetrahedral coordination, and the data are in each case completely consistent with linear M–Y–O groups. Values for the bond lengths (r_g) and bond angles ($\angle_\alpha$) with estimated 2σ uncertainties are as follows: for $Cr(NO)_4$, $r(Cr—N) = 1.763$ (2) Å, $r(N{=}O) = 1.171$ (2) Å (T_d symmetry assumed); for $MnCO(NO)_3$, $r(Mn—N) = 1.717$ (2) Å, $r(Mn—C) = 1.947$ (7) Å, $r(N{=}O) = 1.167$ (2) Å, $r(C{=}O) = 1.145$ (6) Å, $\angle NMnN = 112.5$ (43)°, $\angle CMnN = 106.2$ (49)° (C_{3v} symmetry assumed); for $Fe(CO)_2(NO)_2$, $r(Fe—N) = 1.688$ (3) Å, $r(Fe—C) = 1.883$ (3) Å, $r(N{=}O) = 1.171$ (4) Å, $r(C{=}O) = 1.140$ (4) Å, $\angle NFeN = 114.2$ (62)°, $\angle CFeN = 108.4$ (13)°, $\angle CFeC = 110.2$ (25)° (C_{2v} symmetry assumed). These compounds, together with $Co(CO)_3NO$ and $Ni(CO)_4$ studied earlier, comprise a series of five isoelectronic molecules that allows unusual insight into the nature of the bonding between transition metals and nitrosyl and carbonyl ligands. Changes in bond lengths of the type $\Delta r(M\text{–}C)$ and $\Delta r(M\text{–}N)$ throughout the series are found to correspond to a generally increasing bond order in both cases as the atomic number of the metal increases, while at the same time the total bond order of the metal bonds in each compound changes very little. These metal–ligand bond order changes are interpreted in terms of a redistribution of $d\pi\text{–}\pi^*$ back-bonding and, together with the M–Y distances themselves, are consistent with the NO ligand being a much better electron acceptor than the CO ligand.

Introduction

The nature of the bonding between transition-metal atoms and ligands such as CO and NO is a matter of considerable current interest. These bonds are usually regarded as having a σ component arising from donation of an unshared electron pair on the carbon or nitrogen atom and a "back-bonding" π component arising from combination of an appropriate filled metal orbital with an antibonding orbital on the ligand. The interesting questions concern the relative amounts of the two bond components and the relative abilities of CO and NO to participate in back-bonding. Information bearing on these questions includes bond strengths, charge distributions, and molecular structure as deduced from a variety of experiments and from theoretical calculations.

One approach to an understanding of the bonding in the transition-metal carbonyls and nitrosyls involves comparisons of

---

(1) (a) Oregon State University. (b) University of Texas. Present address: Physics Department, University of Delaware, Newark, DE 19711. (c) University of Texas. Present address: University of California, Los Alamos Scientific Laboratory, Los Alamos, NM 87545.

0020-1669/85/1324-2766$01.50/0 © 1985 American Chemical Society